Optimal arrangement of heliostat field based on simulated annealing algorithm

Zhanghan Li [1, *], Shuming Gan[2]

[1]School of Automation, Guangdong University of Technology, GuangZhou, 510006, China

[2]School of Materials and Energy, Guangdong University of Technology, GuangZhou, 510006, China

* Corresponding Author Email: lzhgdut2013@163.com

Abstract. In this study, a simulated annealing algorithm is proposed as an optimisation method for the mirror arrangement of heliostat mirrors in a tower solar thermal power plant. Firstly, the optimal number and position of heliostats in the whole mirror field in radial staggered layout (EB unobstructed layout) were solved using simulated annealing method. Then further optimisation, i.e. changing the mirror width, mirror height and mounting height of the heliostats and solving for the optimal number and position of heliostats using simulated annealing again, resulted in an increase in the number of heliostats in the optimised mirror field by 77.92% but a decrease in the total area by 18.77%, and an increase in the average annual thermal power output per unit area of the mirrors by 4.76%. Therefore, this result shows that the heliostat field optimised using the simulated annealing algorithm has a higher efficiency and a smaller footprint.

Keywords: Tower solar thermal, Heliostat, Simulated annealing algorithm, Optimal arrangement.

1. Introduction

In response to global climate change and environmental pollution, China is actively taking action to achieve the goals of "carbon peaking" and "carbon neutrality" [1]. In this important context, the development and wide application of new energy technologies have become particularly critical. Among them, tower solar thermal power generation technology, as a low-carbon and environmentally friendly clean energy technology, has great potential and is rapidly emerging in the field of power generation.

The heliostat is the core component of the tower solar thermal power plant, which acts similar to a magnifying glass to focus the solar rays onto the heat absorber and convert the light energy into high-temperature heat energy, thus realising the efficient conversion of clean energy [2]. The heliostat field, on the other hand, consists of a large number of heliostats and is the core and key component of the whole power plant. The layout and design quality of the heliostat mirror field directly affect the performance, efficiency and economy of the power plant [3]. In order to design a more reasonable mirror field, Gao Bo [4] and others proposed a method of optimal layout of the heliostat mirror field based on adaptive gravitational search algorithm, and Sun Hao [5] proposed a research and optimisation method of the heliostat mirror field layout based on the mixed strategy whale optimisation algorithm. In this paper, the problem of optimal layout of fixed-sun mirror field is combined with intelligent optimisation algorithm to propose a flexible and efficient scheduling method.

2. Arrangement and improvement of fixed-sun mirror field based on SA

2.1. Mirror Field Layout Theory

The radial staggered layout method is a common layout strategy when performing optimised design of tower solar power fields. As the radius increases, the heliostat field usually shows a trend from dense to sparse layout, which means that there may be a lot of underutilised space in the rear heliostat area[8].The EB layout is a variant of the radial staggered layout method, the main principle

of which is to ensure that the sun is efficiently focused on the heat absorbing towers or photovoltaic cells. It uses a special arrangement of heliostat mirrors to minimise shadows and shading. By arranging the mirrors closely together, this energy loss is minimised, ensuring that as much of the solar rays as possible are efficiently focused onto the light-focusing tower, thereby increasing the efficiency of energy collection.In order to achieve an optimal mirror field layout, it is necessary to minimise cosine efficiency, shadow obscuration efficiency and truncation loss simultaneously. This means that it is necessary to arrange the heliostats as closely as possible in the layout of the mirrors while solving the problem of mutual shading between the heliostats.

In the following Figure 1, some symbols are used in this paper to represent the different parameters: H_s, on the other hand, denotes the height of the heliostat, D_M represents the diagonal length of the heliostat, and W_s the width of the heliostat. Starting from the ring closest to the heat-absorbing tower, the distance between individual rings is labelled as the radial distance $\triangle R$. The angle between the lines connecting the centres of neighbouring heliostats on the same ring and the origin of the coordinates is known as the azimuthal angle $\triangle \alpha$, and the distance between the centres of neighbouring heliostats is known as the azimuthal distance $\triangle A$. In the layout of the heliostat field, since the heliostats themselves can be rotated, the layout representation can be simplified by using an equivalent characteristic circle. In the top view, the diameter of this eigencircle is equal to the diagonal length of the heliostat D_M, while in the main view, the diameter of the eigencircle is equal to the height of the heliostat H_s. The eigencircle can be rotated by the centre of the heliostat itself[9].

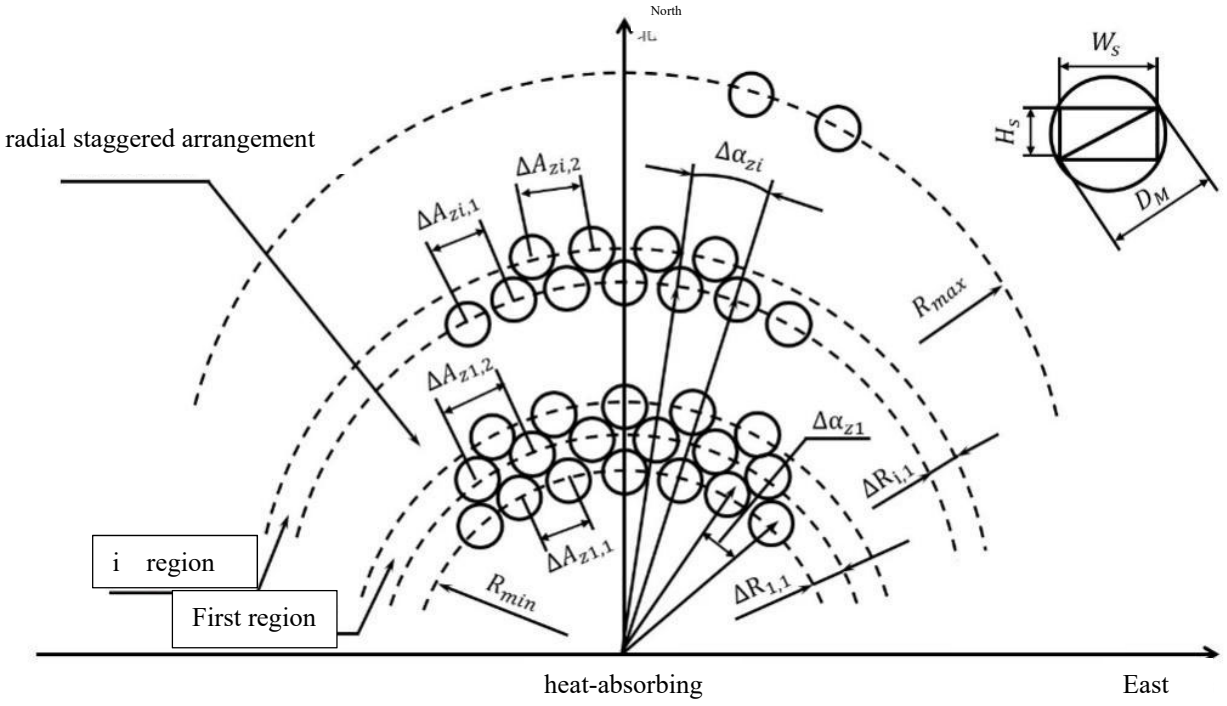

Figure 1. EB Layout Schematic

For better illustration, this paper will take quadrants 1 and 2 of the plane coordinate system as an example, and quadrants 3 and 4 will be calculated in the same way. As shown in the figure above, the 3D spatial coordinate system is projected onto the plane and the position of the heat absorption tower is located at the origin of the coordinates. The distance between the first ring and the heat-absorbing tower is the shortest acceptable distance, denoted as R_{min}, which represents the shortest distance from the heat-absorbing tower to the heliostat. And R_{max}denotes the maximum radius of the heliostat field, i.e., the farthest distance from the heat-absorbing tower to the heliostat. The whole heliostat field is divided into different heliostat ring regions according to different radii, and the directions on the 1st ring of each region are equally spaced, viz:

$$\triangle A_{z1,1} = \triangle A_{z2,1} = \cdots = \triangle A_{zi,1} = A_{sf} \cdot W_S \tag{1}$$

Where: $\triangle A_{zi,1}$ denotes the directional spacing of the 1st ring of the i region. A_{sf} is the azimuthal spacing factor, which is generally related to the height of the tower, and is generally taken as 2.

Neighbouring heliostats in each region have the same azimuth angle, and the azimuthal spacing of neighbouring heliostats on rings other than the first ring can be calculated from the heliostat azimuth angle $\triangle \alpha_{z,i}$. The heliostat azimuth $\triangle \alpha_{z,i}$ can be calculated from the radius $R_{i,1}$ and the orientation spacing $\triangle A_{zi,1}$ of the first row as follows:

$$\triangle A_{zi,j} = 2R_{i,j} \cdot \sin\frac{\triangle \alpha_{z,i}}{2} \tag{2}$$

$$\triangle \alpha_{z,i} = 2\arcsin\frac{\triangle A_{zi,1}}{2R_{i,1}} \tag{3}$$

Since the azimuths of neighbouring heliostats on individual rings within the same region are the same, it is only necessary to use the azimuth of the first ring $\triangle \alpha_{z,i}$, to derive the number of heliostats $N_{hel,i}$, for all the rings in the region:

$$N_{hel,i} = \frac{2\pi}{\triangle \alpha_{z,i}} \tag{4}$$

As the distance between the heat-absorbing tower and the fixing mirrors increases, the radius of the circle increases accordingly, which leads to an increase in the directional spacing between the fixing mirrors. In order to avoid too sparse arrangement of the heliostats in the region away from the heat absorption tower, the EP layout introduces a hyperparameter named A_{rlim}. The EP layout is designed as a super-parameter. When the orientation spacing of the heliostats between the end ring and the first ring exceeds A_{rlim} in a region in the mirror field, a new mirror field region needs to be started. And to start the i+1th region, the following conditions need to be satisfied:

$$\frac{\triangle A_{zi,k}}{\triangle A_{zi,1}} > A_{rlim} \tag{5}$$

The radial distance of the heliostat at the junction of the neighbouring mirror field regions is constant and is denoted as $\triangle R = DM$. Where $\Delta R_{1,1}$ denotes the radial spacing between the first and the second ring in the 1st region of the mirror field, which is calculated as follows:

$$\Delta R_{1,1} = \sqrt{D_M^2 - (\Delta A_{Z1}/2)^2} \tag{6}$$

Starting at ring 3, it is necessary to determine the shortest radial distance that will not be occluded by ring 1. To calculate this distance, we use the unobstructed geometric mapping method, which is shown schematically below[10].

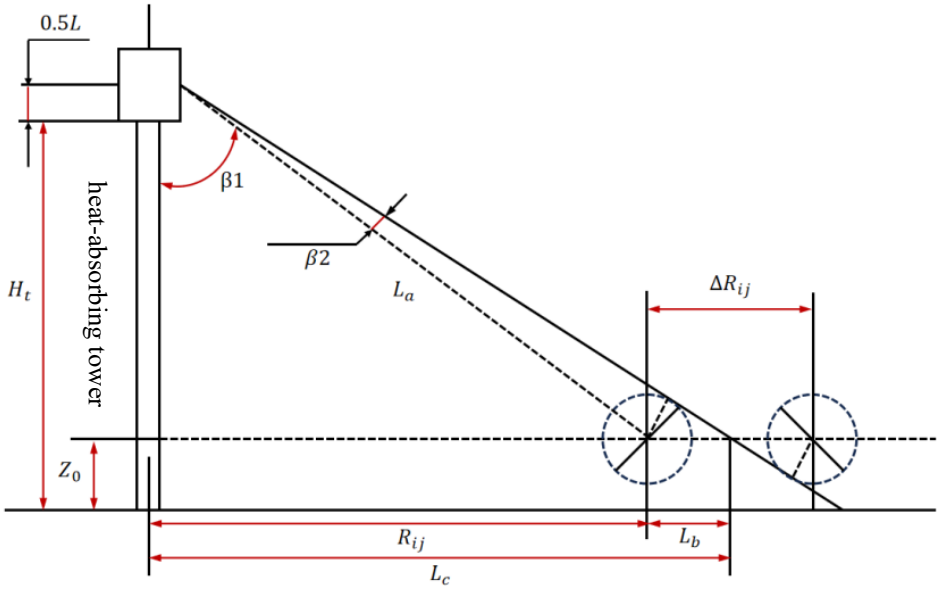

Figure 2. Geometrical calculation of the shortest radial distance

In the Figure 2, β_1 represents the angle of the ray from the centre point of the heat absorber to the front row of heliostats to the y, while β_2 represents the angle of the ray from the centre point of the heat absorber to the midpoint of the line connecting the centres of the front and rear rows of heliostats to the y. Z_0 denotes the fixed height of the heliostats. H_t denotes the optical height of the heat absorbing tower. L denotes the Euclidean distance of the ray from the centre point of the heat absorber to the target heliostat in front of the front row of heliostats. From the centre point of the heat absorber, a tangent line is made along the front row of heliostats until it is tangent to the target heliostat. This tangent line represents the reflected rays of the target sidereal mirror that are not blocked by the front row sidereal mirror. L_a is half the distance between the centre points of the two sidereal mirrors at this point, i.e. half the radial distance. L_b is the sum of the radii of the front row sidereal mirrors, $R_{i,j}$,and L_b. R_0 denotes the radius of the sidereal mirror's circle, which is equal to half the sidereal mirror's height. Based on these geometric relationships, the unobstructed radial distance between the rear row of heliostats and the front row of heliostats can be calculated as follows:

$$L_a = \sqrt{(H_t + 0.5L - Z_0)^2 + R_{i,j}^2} \tag{7}$$

$$\beta_1 = \arcsin\left(\frac{R_{i,j}}{L_a}\right) \tag{8}$$

$$\beta_2 = \arcsin\left(\frac{R_0}{L_a}\right) \tag{9}$$

$$L_c = \tan(\beta_1 + \beta_2) \cdot (H_t - Z_0) \tag{10}$$

$$\Delta R_{i,j} = 2L_b = 2\left(L_c - R_{i,j}\right) \tag{11}$$

2.2. Objective function and constraints under EB (unobstructed) layout

Based on the previous discussion, it is only necessary to set the hyperparameters A_{rlim} and A_{sf} of the EP layout, and then according to the theory of EP layout, we can determine the coordinate positions of all the heliostats. Once these coordinates are obtained, we can combine the vertical height, width W_s, and height H_s of the heliostats, and according to the optical efficiency calculation method, we can obtain the formula for the annual average thermal power output per unit mirror area:

$$\max F = \frac{DNI \sum_{i=1}^{n} A_i \eta_i}{\sum_{i=1}^{n} A_i} \tag{12}$$

$$\eta = \eta_{cos} \cdot \eta_{sb} \cdot \eta_{at} \cdot \eta_{trunc} \cdot \eta_{ref} = f_\eta\left(A_{rlim}, A_{sf}, Z_0, W_s, H_s\right) \tag{13}$$

Where: N is the total number of heliostats ,A_i is the area of the first heliostat.

If it is required that the total average annual thermal power output shall not be less than 60 MW, secondly, the distance between any two heliostats shall be at least five times greater than the width of the heliostats and no heliostats shall be permitted to be placed around the heat-absorbing towers, i.e., within the R_{min} range. In addition to the constraints on the mirror width, mirror height, and mounting height itself, it is also necessary to constrain that the width of the heliostat should normally be no less than its height. The specific constraints are shown below.

$$s.t. \begin{cases} W_S \geq H_S \\ (x_2 - x_1)^2 + (y_2 - y_1)^2 \geq 5 + W_S \\ R_{max}^2 \geq x_i^2 + y_i^2 \geq R_{min}^2 \\ 2 < W_s < 8 \\ 2 < H_s < 8 \\ 2 < Z_0 < 6 \\ DNI \sum_{i=1}^{n} A_i \eta_i \geq 60(MW) \end{cases} \tag{14}$$

2.3. Layout improvement in case of different heights and sizes of heliostats

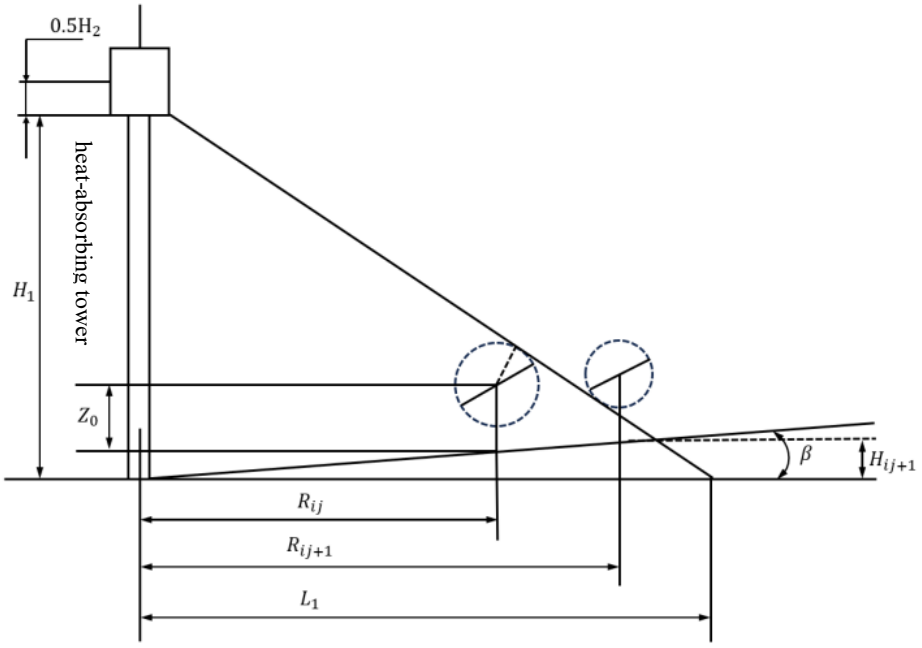

Figure 3. Geometric calculation of the shortest radial distance

A method known as the EB (unobstructed) layout method was used above, which requires the determination of only two hyperparameters A_{rlim} and A_{sf} to compute the coordinates of all the heliographs. The cleverness of this method lies in the reduction of the dimensionality of the parameters, which reduces the time complexity of solving the problem.The geometric method for calculating the shortest radial distance in this layout is shown in Figure 3 above.

Referring to the idea of EB layout, this method is further optimised by considering the case that the mirror width, mirror height and mounting height can be different for different heliostats. We

introduce the tilt angle β and the variation factor A_r, where the tilt angle β denotes the degree of tilt of the mirrors and the variation factor A_r denotes the coefficient by which the mirror widths and mirror heights of the heliostats change with the increase in the number of rings starting from the first heliostat on the first ring, which makes it possible to determine the spatial co-ordinates of all the heliostats of the whole mirror field with the determination of the four parameters only, A_{rlim}、A_{sf}、β and A_r. Once the coordinates of the heliostat are determined, the thermal power output of the heliostat field can be estimated.

Suppose that at different heliostat locations, their vertical distance from the ground remains fixed Z_0 , but the ground will exhibit a slope with an angle of inclination β, but exhibits a slope with an inclination angle of β . For the j+1 ring on the i region, the difference in height between them can be expressed as H_(ij+1), and then the true distance from the ground on this ring Z , can be calculated from Z_0 and H_(ij+1):

$$H_{ij} = R_{ij} \tan \beta \tag{15}$$

$$Z_{ij} = H_{ij} + Z_0 \tag{16}$$

Assuming that the centre coordinate of a previous heliostat is (y_1, z_1) , and the centre coordinate of the heliostat to be solved is (y_2, z_2) , based on the geometrical relationship, we can obtain the characteristic circular equation of the heliostat to be solved and the linear equation of the tangent line as follows:

$$(y - y_2)^2 + (z - z_2)^2 = (0.5H_s)\text{^}2 \tag{17}$$

$$\frac{y}{y_1} = \frac{z}{z_1} = 1 \tag{18}$$

Solving for the geometric relationship gives:

$$R_{ij} = y_2 = \frac{-B - \sqrt{B^2 - 4AC}}{2A} \tag{19}$$

$$\begin{cases} A = -z_1^2 y_1^2 \\ B = 2z_1 y_1 (z_1 - z_0) \\ C = \left(\frac{H_s}{2}\right)^2 (1 + z_1^2 + y_1^2) - (z_1 - z_0)^2 \\ y_1 = \frac{-b - \sqrt{b^2 - 4ac}}{2a} \\ a = a_1^2 \left(\left(\frac{H_s}{2}\right)^2 - y_1^2\right) \\ b = 2y_1 z_1 (z_1 - z_0) \\ c = \left(\frac{H_s}{2}\right)^2 - (z_0 - z_1)^2 \end{cases} \tag{20}$$

After the layout correction, the rest of the calculations are the same as above and will not be repeated.

2.4. Objective function and constraints under EB (improved) layout

The modified EB layout involves hyperparameters including A_{rlim}、A_{sf}，β，A_r, using which the coordinate positions of all heliostats can be determined. With this coordinate information, the annual average thermal power output per unit mirror area is estimated by optical efficiency calculation methods, combining the mirror width W_s, vertical height Z_s and mirror height H_s of

each heliostat. It is important to note that the mirror width W_s , mirror height Z_s and vertical height H_s are no longer fixed values, and detailed calculations are required to determine the specific values for each mirror.

$$\max F = \frac{DNI \sum_{i=1}^{n} A_i \eta_i}{\sum_{i=1}^{n} A_i} \tag{21}$$

$$\eta = \eta_{cos} \cdot \eta_{sb} \cdot \eta_{at} \cdot \eta_{trunc} \cdot \eta_{ref} = f_\eta\left(A_{rlim}, A_{sf}, \beta, A_r, Z_0, W_s, H_s\right) \tag{22}$$

Where: A_i is the area of the first heliostat and N is the total number of heliostats.

$$s.t. \begin{cases} W_S \geq H_S \\ (x_2 - x_1)^2 + (y_2 - y_1)^2 \geq 5 + W_S \\ R_{max}^2 \geq x_i^2 + y_i^2 \geq R_{min}^2 \\ 2 < W_s < 8 \\ 2 < H_s < 8 \\ 2 < Z_0 < 6 \\ DNI \sum_{i=1}^{n} A_i \eta_i \geq 60(MW) \end{cases} \tag{23}$$

After obtaining the objective function and constraints, a simulated annealing algorithm can be used to solve the problem.

3. Results

Figure 4(a)below shows the distribution of the fixed heliograph field in the EB (Shelterless) layout. The value of the objective function is relatively high in the initial phase of iterations, but it gradually and steadily decreases with the increase of the number of iterations, and finally converges to a desirable minimum value. In the optimal solution, the value of the hyperparameter A_{rlim} is 1.72 and the value of the azimuthal spacing factor A_{sf} is 1.9.

Figure 4(b) below shows the distribution of the fixed heliograph field in the EB (improved) layout.After applying the simulated annealing algorithm for the solution, the optimal solution is obtained as shown in Figure 5 above, where the optimal value of the hyperparameter A_{rlim} is 1.5732 and the optimal value of the azimuthal spacing factor A_{sf} is 1.4189.

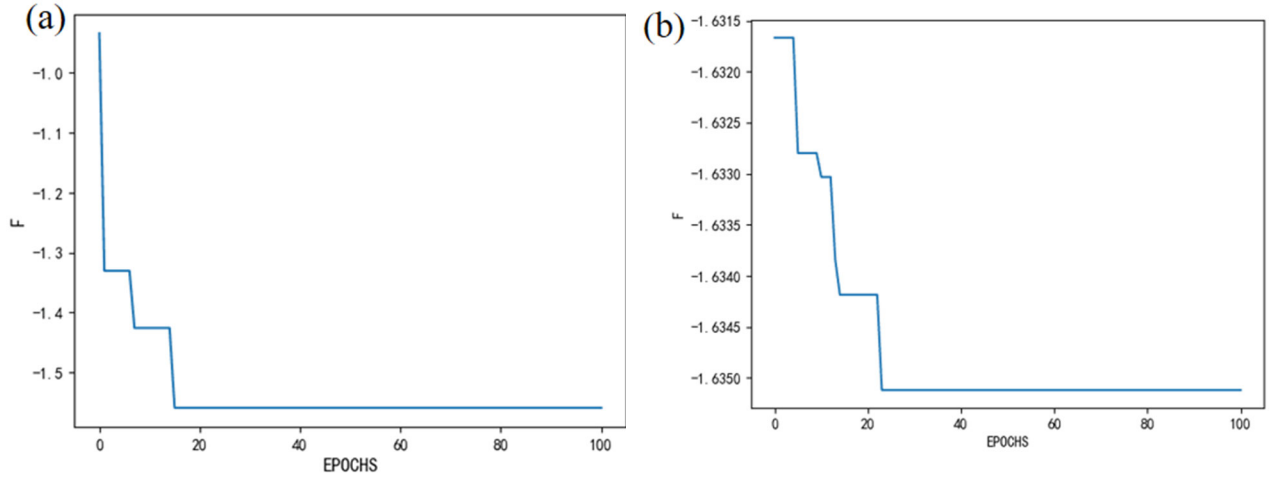

Figure 4. (a) Distribution of the fixed heliograph field in the EB (Shelterless) layout
(b) Distribution of the fixed heliograph field in the EB (improved) layout

The results of the distribution of the fixed heliostat field at the optimal parameters solved using the simulated annealing algorithm in the EB (Shelterless) layout are shown in Figure 5(a).The results

of the distribution of the fixed heliostat field at the optimal parameters solved using the simulated annealing algorithm in the EB (improved) layout are shown in Figure5(b).

Through the iterative optimisation of the simulated annealing algorithm, the heliostats were able to be arranged in an optimal manner to maximise the average annual thermal power output per unit mirror area.

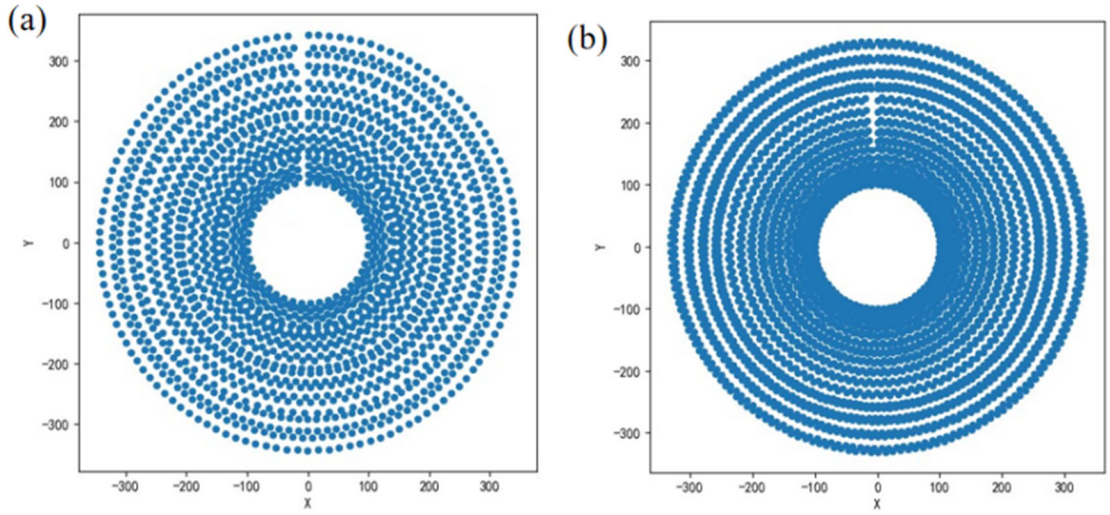

Figure 5. (a) Schematic representation of the heliostat field with EB (Shelterless) layout (b)Schematic representation of the heliostat field with EB (improved) layout

Table 1. Average optical efficiency and output power on the 21st of each month for both layouts

Time	Average optical efficiency		Average cosine efficiency		Average Shadow Occlusion Efficiency Efficiency		Average cut-off efficiency efficiency		Mirror per unit area Average thermal power output	
	Shelterless	improved	Shelterless	improved	Shelterless	improved	Shelterless	improved	Shelterless	improved
21-Jan	0.39	0.41	0.73	0.73	1	1	0.61	0.61	1.33	1.53
21-Feb	0.41	0.42	0.75	0.75	1	1	0.61	0.61	1.48	1.59
21-Mar	0.42	0.43	0.77	0.77	1	1	0.61	0.61	1.61	1.61
21-Apr	0.43	0.44	0.79	0.79	1	1	0.61	0.61	1.71	1.67

Table 2. Annual average optical efficiency and output power for both layouts

layout	Average optical efficiency	Average cosine efficiency	Average Shadow Occlusion Efficiency Efficiency	Average cut-off efficiency efficiency	Average annual thermal power output(MW)	Average thermal power output per unit area of mirror
Shelterless	0.415	0.766	1	0.609	177.461	1.562
improved	0.4283	0.7654	1	0.6136	234.8212	1.6359

Table 3. Design parameters for both layouts

layout	Absorption tower position coordinates	Sunset mirror size (W×H)	Installation height of fixed-sun mirror (m)	Total number of heliostats	Total area of heliostat (m^2)
Shelterless	(0, 0)	7.926×7.852	2.5111	1826	113641.3657
improved	(0, 0)			3249	92283.657

In Tables 1,2 and 3 below, the optical efficiencies of the heliostat mirror field and the calculation results of the relevant parameters are demonstrated. When the hyperparameter A_{rlim} is set to 1.5732

and A_{sf} is set to 1.4189, the annual average thermal power output per unit area of mirror is $1.636kW/m^2$, and the annual average thermal power output is 234.8213 MW. Compared with the results of the EB (Shelterless) layout, the number of heliostat mirrors in the EB (improved) layout is increased to 3249, and the total area of heliostat is $32283.657\ m^2$which increases the number of heliostats by 77.92% but decreases the total area of heliostats by 18.77%, and increases the annual average thermal power output per unit area of mirrors by 4.76%.

4. Conclusions

In this paper, by using the mirror diameter layout method, thousands of unknowns, such as the number of unknown fixed-sun mirrors and their coordinates, are completely represented by fewer unknowns, which reduces the dimensionality of the decision variables, and thus reduces the time complexity of the solution problem. Moreover, the simulated annealing method is used as a nonlinear optimisation method, which is capable of solving complex nonlinear problems without information about the gradient of the objective function. This method is well suited for problems where the derivative information needs to be ignored and is easy to implement. However, when different sizes of heliostats are allowed to be used, there may be some limitations in this paper when only the case of inclined planes is considered. This is because in practice, different sizes of heliostats may be suitable for different situations or tasks. For example, a tilted plane is suitable for some specific solar tracking applications, but in other scenarios a different type of heliostat may be required, such as a spherical or refractive type.

References

[1] Fu CuiXiao, Zhuang Jun, Zheng Yi. Analysis of key technology assessment in the field of carbon peaking and carbon neutrality[J]. New Energy Science and Technology,2023,4(01):6-11.

[2] PENG Jing,SHI Tao. Road design of fixed-sun mirror field for tower solar thermal power station[J]. Southern Energy Construction,2020,7(02):70-74.

[3] SUN Hao,GAO Bo,LIU Jianxing. Research on the layout of heliostat mirror field for tower solar power station[J]. Power Generation Technology,2021,42(06):690-698.

[4] Gao Bo,Liu Jianxing,Sun Hao,et al. Optimal arrangement of heliostat mirror field based on adaptive gravitational search algorithm[J]. Journal of Solar Energy, 2022, 43(10):119-125.

[5] Sun H. Research on the layout and optimisation of heliostat mirror field based on mixed strategy whale optimisation algorithm[D]. Lanzhou Jiaotong University,2022.

[6] Zhang Wanju,Yao Kaixue,He Yong et al. Identification model of oil storage tank displacement based on simulated annealing algorithm[J]. Computer Application and Software,2023,40(07):300-304.

[7] ZHENG Xin, SHU Qinglin, SU Zhaoguang, et al. A new method for modelling composite point dams in Quliu River based on simulated annealing[J]. Broken block oil and gas field, 2023, 30(1):114-119.

[8] Cheng S-L. Research on optimal design of tower power plant mirror field layout based on optical efficiency[D]. Hefei University of Technology [2023-09-18].

[9] CHENG Xiaolong,YIN Yanguo,MA Shaobo. Research on the optimal design of the layout of the fixed-sun mirror field of tower power station[J]. Energy and Environment, 2018(2):4.

[10] Deng Libao, Wu Yiran, Guo Su. Layout of elliptical heliostat mirror field based on decomposed multi-objective evolution[J]. Journal of Zhengzhou University: engineering edition, 2020, 41(5):7.